e_π^L/e_σ^L, the order in terms of decreasing π-acceptor ability is C_2H_4 > $AsPh_3$ > PPh_3 > PEt_3 > NMe_3 > Cl. This order of normalized π-acceptor ability places chloride as a poorer π acceptor than the amine, the position it occupies in the high-oxidation-state "Werner" complexes.

Acknowledgment. The support of this research by the National Science Foundation is gratefully acknowledged.

Registry No. PPh_3, 603-35-0; $AsPh_3$, 603-32-7; $[Pr_4N][PtCl_3PPh_3]$, 19508-39-5; $[Pr_4N][PtCl_3AsPh_3]$, 102493-30-1; $Pt_2Cl_4(PPh_3)_2$, 15349-80-1; $Pt_2Cl_4(AsPh_3)_2$, 39539-17-8.

Contribution from the Laboratoire de Spectrochimie du Solide (LA 302), Université Paris VI, 75230 Paris Cedex 05, France

ESR and ENDOR Study of the Electronic Structure of the Radical Anion $[[CH_3N(PF_2)_2]_3Co_2(CO)_2]^-$

F. Babonneau* and J. Livage

Received November 26, 1985

The ESR spectrum of the radical anion $[[CH_3N(PF_2)_2]_3Co_2(CO)_2]^-$ indicates complete delocalization over the two cobalt sites even at 4 K. The unpaired electron is in the intermetallic σ^* molecular orbital, mainly localized onto the cobalt orbitals: $\rho(Co,d_{z^2})$ = 0.38, and $\rho(Co,4s)$ = 0.006-0.013. The hyperfine couplings with the phosphorus and fluorine nuclei show a little extension of the unpaired electron density on the equatorial fluorophosphine ligands. ENDOR experiments were undertaken: a dipolar coupling between the unpaired electron and the methyl protons is revealed. Other proton signals appeared, which were assigned to one or several protons located on the amino groups. A fluorine ENDOR spectrum was also obtained, which confirmed the hyperfine coupling values first deduced from the ESR spectra. Extended Hückel calculations are presented that are consistent with the description of the ground-state molecular orbital deduced from ESR and ENDOR experiments.

The electronic structure of polynuclear transition-metal complexes is of current interest.[1-6] ESR appears to be a very powerful technique for studying such complexes when they are paramagnetic. Otherwise, in the case of diamagnetic compounds, it is sometimes possible to get a paramagnetic radical ion through redox reactions. ESR then gives indirect information on the HOMO or LUMO of the parent neutral complex.[7-9] However, the metal-metal bond is often so weak that redox reactions lead to the dissociation of the complex. It would be therefore quite interesting to synthesize bridging ligands that are able to stabilize the metal-metal bond toward redox reactions. Stable radical ions can then be obtained and spectroscopic studies easily performed.[10] Dinuclear complexes with bis(difluorophosphino)alkylamino bridging ligands have been recently synthesized from cobalt,[10-12] iron,[13-15] and molybdenum[16] carbonyl compounds. The cobalt dinuclear derivative $[CH_3N(PF_2)_2]_3Co_2(CO)_2$ undergoes a reversible one-electron reduction, giving rise to a radical anion that remains stable under an inert atmosphere.[17]

An ESR study of the paramagnetic $[[CH_3N(PF_2)_2]_3Co_2(CO)_2]^-$ radical anion was recently published.[18] It showed that the unpaired electron was equally delocalized over the two cobalt units in a σ^* metal-metal molecular orbital. The complex then belongs to class III of the mixed-valence compounds, according to the classification suggested by Robin and Day.[19] Some information about electron delocalization over the ligands were obtained from the hyperfine structure of the spectrum. But, due to the line width, some hyperfine couplings were not resolved.

In this paper, we present an ENDOR study giving more details about the different hyperfine interactions together with LCAO-MO calculations of the electronic structure of the complex.

Experimental Results

A. ESR Results. X- and Q-band ESR spectra have already been published.[18] They were analyzed by trial and error comparison with simulated spectra.[20] They show that, even at 4 K, the unpaired electron remains equally delocalized over the two cobalt units.

The following **g** tensor values were determined from both room- and low-temperature spectra assuming an axial symmetry: $g_\perp$ = 2.03; $g_\parallel$ = 2.00; g_0 = 2.025.

The hyperfine structure of the ESR spectra also provided information about the couplings between the unpaired electron and some nuclei having a nonzero nuclear spin. For cobalt, $|A_0(Co)|$ = 18 G, $|A_\perp(Co)|$ = 48 G, and $|A_\parallel(Co)|$ = 38 G; for phosphorus, $|A_0(P)|$ = 42.7 G, $|A_\perp(P)|$ = 42.7 G, and $|A_\parallel(P)|$ = 42.7 G; for fluorine, $|A_0(F)|$ = 5.3 G.

(1) Symons, M. C. R.; Bratt, S. W. *J. Chem. Soc., Dalton Trans.* **1979**, 1739.
(2) Peake, B. M.; Rieger, P. H.; Robinson, B. H.; Simpson, J. *J. Am. Chem. Soc.* **1980**, *102*, 156.
(3) Cotton, F. A.; Pedersen, E. *J. Am. Chem. Soc.* **1975**, *97*, 303.
(4) Kawamura, T.; Fukamachi, K.; Hayashida, S. *J. Chem. Soc., Chem. Commun.* **1979**, 94S.
(5) Strouse, C. E.; Dahl, L. F. *Discuss. Faraday Soc.* **1969**, *47*, 93.
(6) Hayashida, S.; Kawamura, T.; Yanezawa, T. *Inorg. Chem.* **1982**, *21*, 2235.
(7) Cotton, F. A.; Pedersen, E. J. *J. Am. Chem. Soc.* **1975**, *97*, 303.
(8) Bratt, S. W.; Symons, M. C. R. *J. Chem. Soc., Dalton Trans.* **1977**, 1314.
(9) Kawamura, T.; Hayashida, S.; Yonezawa, T. *Chem. Lett.* **1980**, 517.
(10) King, R. B. *Acc. Chem. Res.* **1980**, *13*, 243.
(11) Newton, M. G.; King, R. B.; Chang, M.; Pantaleo, N. S.; Gimeno, J. *J. Chem. Soc., Chem. Commun.* **1977**, 531.
(12) King, R. B.; Gimeno, J.; Lotz, T. J. *Inorg. Chem.* **1978**, *17*, 2401.
(13) King, R. B.; Gimeno, J. *Inorg. Chem.* **1978**, *17*, 2390.
(14) Newton, M. G.; King, R. B.; Chang, M.; Gimeno, J. *J. Am. Chem. Soc.* **1977**, *99*, 2802.
(15) King, R. B.; Lee, T. W.; Kim, J. H. *Inorg. Chem.* **1983**, *22*, 2964.
(16) King, R. B.; Shimura, M.; Brown, G. M. *Inorg. Chem.* **1984**, *23*, 1398.
(17) Chaloyard, A.; El Murr, N.; King, R. B. *J. Organ. Chem.* **1980**, *188*,C 13.
(18) Babonneau, F.; Henry, M.; El Murr, N.; King, R. B. *Inorg. Chem.* **1985**, *24*, 1946.
(19) Robin, M. D.; Day, P. *Adv. Inorg. Chem. Radiochem.* **1967**, *10*, 248.
(20) For analysis of the ESR spectra, a simulation programm REPELEC was used on the basis of a second-order perturbation solution of the spin Hamiltonian.

0020-1669/86/1325-2741$01.50/0

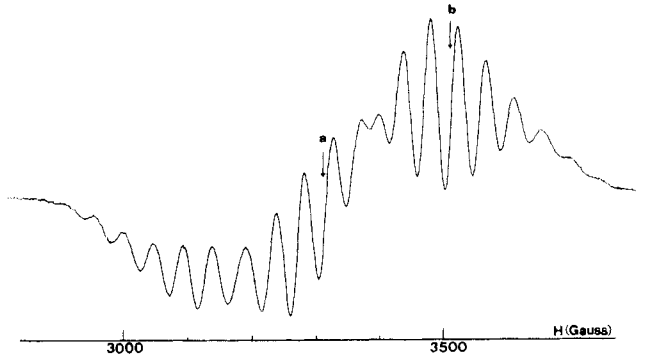

Figure 1. ESR spectrum of $[Co_2(CO)_2[CH_3N(PF_2)_2]_3]^-$ in THF at 4 K.

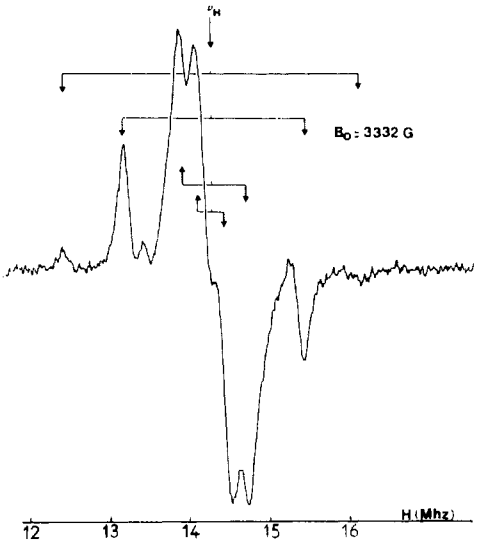

Figure 2. ENDOR spectrum from 10 to 20 MHz of $[Co_2(CO)_2[CH_3N(PF_2)_2]_3]^-$ in THF at 4 K.

The fluorine hyperfine interactions were not resolved in the anisotropic low-temperature spectrum because of the rather large line widths.

B. ENDOR Results. ESR spectra gave complete information about the hyperfine interactions between the unpaired electron and the cobalt and phosphorus nuclei. The splitting of about 5 G between each line of the isotropic room-temperature spectrum was attributed to hyperfine interactions with the 12 magnetically equivalent fluorine nuclei. But in the radical anion $[[CH_3N(PF_2)_2]_3Co_2(CO)_2]^-$, such couplings could also result from nitrogen nuclei and, less likely, from hydrogen nuclei. ENDOR experiments of this radical anion were thus performed in order to confirm such an assumption.

A concentrated solution of the radical anion in tetrahydrofuran ($c \cong 0.1$ M) was used, and the spectra were recorded at 4 K. In the case of strongly anisotropic ESR spectra, ENDOR experiments can be performed for different specific orientations of the magnetic field, leading to ENDOR spectra that look like "single-crystal spectra".[21] An analysis of such spectra is then quite easy. In the case of our radical anion, the anisotropy of both **g** and **A** tensors was too small to allow such an analysis. Whatever the observed ESR line could be, the ENDOR spectrum remains almost unchanged and then reflects all magnetic field orientations. No ENDOR spectrum was observed below 10 MHz. Beyond this value and up to 100 MHz several lines appear, and three frequency ranges can be distinguished from 10 to 20 MHz (Figure 2), from 20 to 50 MHz (Figure 3), and from 50 to 100 MHz (Figure 4).

From 10 to 20 MHz: The Proton Resonance Spectrum. Over this frequency range, the ENDOR spectrum exhibits four pairs of lines. The spectrum shown in Figure 2 was obtained for an observed magnetic field of 3332 G (point a in Figure 1). All pairs

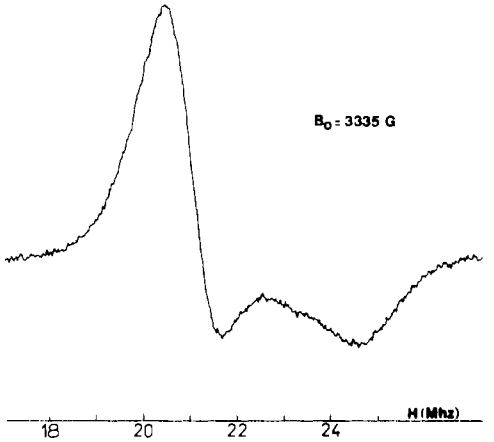

Figure 3. ENDOR spectrum from 20 to 30 MZh of $[Co_2(CO)_2[CH_3N(PF_2)_2]_3]^-$ in THF at 4 K.

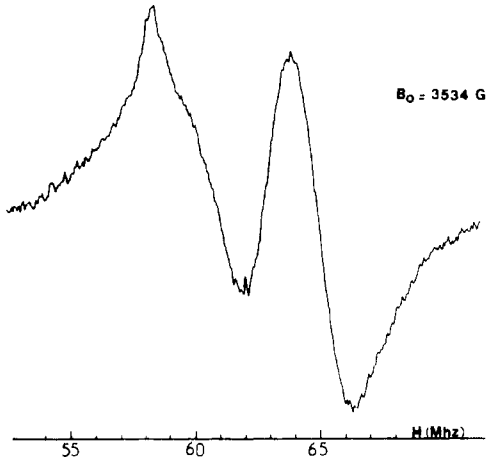

Figure 4. ENDOR spectrum from 50 to 100 MHz of $[Co_2(CO)_2[CH_3N(PF_2)_2]_3]^-$ in THF at 4 K.

are centered around the proton nuclear resonance frequency ν_H: they are undoubtedly due to the interaction between the unpaired electron and the proton nuclei. The observed couplings are 0.4, 0.8, 2.3, and 3.8 MHz.

According to the structural data,[22] the only protons present in the radical anion, those of the methyl groups, are located about 6 Å away from the cobalt nuclei. Because of this large distance, the transferred hyperfine couplings via chemical bonds should be very small[23] and the observed values should arise mainly from dipolar interactions.

For a distance of 6 Å, the dipolar term can be estimated to be around 0.4 MHz for the parallel orientation and 0.8 MHz for the perpendicular one. It seems then quite reasonable to assume that the observed values of 0.4 and 0.8 MHz result from the dipolar interaction of the unpaired electron with the proton nuclei of the methyl groups.

A straightforward assignment of the stronger couplings at 2.3 and 3.8 MHz is not obvious. We can consider them as parallel and perpendicular hyperfine parameters due to one or several protons located in the cage built by the three bridging ligands. These low coupling values indicate that this proton is not in close contact with the cobalt nuclei. Thus the anisotropic term would be essentially a purely dipolar term:

(21) Gersmann, H. R.; Swallen, J. D. *J. Chem. Phys.* **1962**, *36*, 3221.
(22) Newton, M. G.; Pantaleo, N. S.; King, R. B.; Lotz, T. J. *J. Chem. Soc., Chem. Commun.* **1978**, 514.
(23) Van Willigen, H. *J. Magn. Reson.* **1980**, *39*, 37.
(24) Atherton, N. M.; Shackleton, J. F. *Mol. Phys.* **1980**, *39*, 1471.
(25) Freeman, A. J.; Watson, R. E. *Magnetism* Rado, G. T., Suhl, H., Eds.; Academic: New York, **1965**; Vol. II.A, p 167.
(26) Morton, J. R.; Preston, K. F. *J. Magn. Reson.* **1978**, *30*, 577.
(27) Herman, F.; Skillman, S. *Atomic Structure Calculations*; Prentice-Hall: Englewood Cliffs, NJ (1963).

$$a_\perp = a_0 - a_d \quad (1a)$$

$$a_\parallel = a_0 + 2a_d \quad (1b)$$

a_0 is the isotropic term, positive or negative; a_d is the dipolar one, always positive. Two possibilities have to be considered for the signs of the couplings: (i) $a_\perp = +2.3$ MHz, $a_\parallel = +3.8$ MHz; (ii) $a_\perp = -2.3$ MHz $a_\parallel = +3.8$ MHz. The other ones are unrealistic. The first possibility (i) leads to $a_0 = +2.8$ MHz and $a_d = +0.5$ MHz. Such a dipolar value corresponds to a cobalt–proton distance of about 5.5 Å. With such a large distance, the isotropic term would not arise from a Fermi contact term but rather from spin-polarization terms and thus would be negative. This first assumption ($a_\perp = +2.3$ MHz, $a_\parallel = +3.8$ MHz) might be wrong. The second possibility ($a_\perp = -2.3$ MHz, $a_\parallel = +3.8$ MHz) leads to $a_0 = -0.3$ MHz and $a_d = +2.0$ MHz. The estimated cobalt-proton distance is then 3.4 Å. The structural data of the neutral parent complex[22] reveal that the nitrogen nuclei of the amino groups are located at an average distance of 3.3 Å from the cobalt nuclei. It seems then reasonable to assume that at least one proton is located on the nitrogen nucleus of an amino group. With such an assumption, a low negative value is expected for the isotropic term. This is quite consistent with the calculated a_0 value. An exchange process of the proton between the three amino groups must not be ignored: the difference between the parallel and perpendicular components just indicates that the proton stays for at least 1 μs on an amino group. Electrochemical studies have already suggested that small cations such as Li^+ and H^+ could be trapped between the two cobalt sites.[17]

The ENDOR central line that can be seen around the free proton resonance frequency should correspond to the so-called "matrix line". It arises from the coupling with all the protons located far from the unpaired electron, probably those of the tetrahydrofuran solvent.

From 20 to 30 MHz: The Fluorine Resonance Spectrum. Over this frequency range, the observed spectrum is shown in Figure 3 for an observer of 3332 G (point a on Figure 1). As the observer field B_0 increases, this signal shifts toward higher frequencies. Its shape remains unchanged. The amplitude of this shift may allow the identification of the nucleus from which the signal arises. ENDOR lines for a nucleus n of spin $^1/_2$ are, in a first approximation, centered on $|A/2 + \nu_n|(\nu^+)$ or $|A/2 - \nu_n|(\nu^-)$ where A is the hyperfine coupling and ν_n is the resonance frequency for the nucleus n. When the observer field B_0 varies, ν_n varies and the lines shift. A plot of the line position vs. the observer value B_0 should give a straight line, the slope of which is given by $g_n\beta_n/h$, where g_n is the g factor of the nucleus n, β_n is the nuclear magneton, and h is the Planck's constant. In our case, a slope of 3.9 MHz/kG is obtained, which can only result from proton (4.3 MHz/kG) or fluorine (4.0 MHz/kG) hyperfine interactions. In both cases, the signal should be a ν^+ signal centered around $\nu_n + A/2$. If a coupling with the protons is assumed, an hyperfine interaction of about 12.5 MHz is obtained. With the fluorine, the hyperfine interaction would be around 14.0 MHz. This last value is the only one to be acceptable. It agrees quite well with our ESR results. From the isotropic spectrum at room temperature, an hyperfine coupling of 5.3 G, about 15 MHz, was assumed for each of the 12 magnetically equivalent fluorine nuclei.

All these considerations suggest that the ENDOR spectrum around 20 MHz arises from the interaction of the unpaired electron with the fluorine nuclei.

We have to notice that only the ν^+ transition appears in the fluorine spectrum. This could be explained by the various relaxation processes involved in ENDOR experiment.[28]

As mentioned above, the ENDOR spectrum reflects all the magnetic field orientations, and it seems quite reasonable to assign the low-frequency signal to the perpendicular orientation and the high-frequency signal to the parallel one so that $A_\perp(F) = 14.1$ MHz ≅ 5.0 G and $A_\parallel(F) = 22.3$ MHz ≅ 8.0 G. These values are in agreement with the isotropic value $A_0(F) \cong 5.3$ G given by the room-temperature ESR spectrum.

Table I. Hyperfine Couplings in the Radical Anion $[[CH_3N(PF_2)_3]_3Co_2(CO)_2]^-$

	cobalt	phosphorus	fluorine
10^4A_0, cm^{-1}	17	40.4	5
$10^4A_\perp$, cm^{-1}	45.5	40.5	4.7
$10^4A_\parallel$, cm^{-1}	35.5	39.9	7.5

From 50 to 100 MHz: The Cobalt and Phosphorus Resonance Spectra. Over this frequency range, the ENDOR spectrum appears rather complex and slightly varies with the observer B_0. The spectrum is shown in Figure 4 for $B_0 = 3534$ G (point b in Figure 1). Its interpretation is not obvious: for such resonance frequencies, ENDOR lines are centered around $A/2$ rather than around ν_n. So, they should result from hyperfine couplings ranging between 35 and 50 G, as found by ESR for the phosphorus and cobalt nuclei. The hyperfine interactions between the unpaired electron and the phosphorus and cobalt nuclei were very well resolved on ESR spectra so that it does not seem to be useful to undertake a complete interpretation of the complex ENDOR spectra.

This ENDOR study of the radical anion $[Co_2(CO_2)(NCH_3(PF)_2)_3]^-$ complements perfectly the ESR one; it clearly shows the anisotropic hyperfine interactions with fluorine and hydrogen, which were not resolved on ESR spectra because of the rather large line widths. No signal arising from hyperfine interactions with the nitrogen nuclei can be seen. The resonance frequency should be too low, 1 MHz for a 3500-G field. As for the hyperfine couplings, isotropic and dipolar interactions should not exceed 0.5 MHz each.

Discussion

Both ESR and ENDOR studies of the radical anion $[[NCH_3(PF_2)_2]_3Co_2(CO)_2]^-$ gave significant information about the hyperfine interactions between the unpaired electron and the two cobalt nuclei, the six phosphorus nuclei, and the 12 fluorine nuclei.

In a preliminary paper,[18] we concluded that the unpaired electron was in the σ^* orbital of the cobalt–cobalt bond built on the antibonding combination of the d_{z^2} orbitals of each cobalt atom. It would be interesting to improve this description by using the experimental data reported in Table I.

Unpaired Electron Distribution on Cobalt Atomic Orbitals. The unpaired electron density on a cobalt d_{z^2} orbital, $\rho(Co,d_{z^2})$, for the radical anion $[Co_2(CO)_2[NCH_3(PF_2)_2]_3]^-$ can be correlated with the cobalt hyperfine splitting tensor:

$$A_\parallel(Co) = A(Co) + \frac{4}{7}\rho(Co,d_{z^2})\,P(Co,d_{z^2}) - \frac{1}{7}P(Co,d_{z^2})\,\Delta g_\perp \quad (2a)$$

$$A_\perp(Co) = A(Co) - \frac{2}{7}\rho(Co,d_{z^2})\,P(Co,d_{z^2}) + \frac{15}{14}P(Co,d_{z^2})\,\Delta g_\perp \quad (2b)$$

$A(Co)$ is the isotropic coupling term for the cobalt nucleus. $P(Co,d_{z^2})$ is the anisotropic splitting constant for a cobalt nucleus with a single unpaired electron completely localized in the $3d_{z^2}$ orbital. The last term arises from second-order effects due to unquenched orbital angular momenta of electrons. Any mixing of a $4p_z$ atomic orbital in the ground-state molecular orbital was ignored. A survey of the literature shows some disagreement concerning the P value. P is defined as $g_e g_n \beta_e \beta_n \langle r^{-3}\rangle$; β_e and β_n are the Bohr and nuclear magnetons, and g_e and g_n are the electronic and nuclear g factors. Numerical calculations for $\langle r^{-3}\rangle$ depend on the choice of the atomic wavefunctions. Freeman and Watson have calculated $\langle r^{-3}\rangle$ for several transition metal ions, using Hartree–Fock free-ion wave functions.[25] For Co^0, $\langle r^{-3}\rangle = 4.79$ au so that $P = 201 \times 10^{-4}$ cm^{-1}. Morton and Preston did not agree with the choice of Hartree–Fock functions.[26] Using Hartree–Fock–Slater atomic orbitals of Herman and Skillman,[27] they proposed a P value of 282×10^{-4} cm^{-1} for a ^{59}Co nucleus. Most studies published in the literature on Co^0 complexes are based on the P value given by Morton and

(28) Abragam, A.; Bleaney, B. *Résonance Paramagnétique Electronique des Ions de Transition*; Bibliothèque des Sciences et Techniques Nucléaires: Paris, 1971.

Preston. Therefore we took $P = 282 \times 10^{-4}$ cm^{-1} in order to be able to compare our results with previous ones.

Parts a and b of eq 1 only give reasonable calculations for $A_\parallel$ positive and $A_\perp$ negative, respectively, leading to an unpaired electron density on the cobalt d_{z^2} atomic orbital and an isotropic hyperfine coupling constant estimated as $\rho(Co,d_{z^2}) = 0.38$ and $A(Co) = 24 \times 10^{-1}$ cm^{-1} respectively. In our preliminary paper,[8] the unpaired electron density $\rho(Co,d_{z^2})$ was overestimated because second-order effects in eq 1 were not taken into account.

The isotropic cobalt hyperfine coupling constant arises from the 4s contribution in the ground-state orbital, which is allowed from symmetry considerations, as well as from spin polarization of the filled 1s, 2s, and 3s orbitals. Assuming that this least term is proportional to $\rho(Co,d_{z^2})$, the unpaired electron density in the cobalt 4s atomic orbitals $\rho(Co,s)$ may be evaluated as

$$A(Co) = Q_I(Co)\ \rho(Co,d_{z^2}) + Q_V(Co)\ \rho(Co,s)$$

$Q_V(Co)$ is a Fermi contact term arising from an unit 4s unpaired electron density. According to Morton and Preston,[26] $Q_V(Co) \cong 1980 \times 10^{-4}$ cm^{-1} and $Q_I(Co)$ is the inner-shell spin-polarization term. It was estimated as $(-94$ to $-131) \times 10^{-4}$ cm^{-1}.[2,6] With such numerical values, the 4s unpaired electron density may be evaluated as

$$\rho(Co,s) = 0.006\text{–}0.013$$

The unpaired electron density is mainly localized on the cobalt orbitals, about 76% in the $3d_{z^2}$ orbitals and 2% in the 4s orbitals. From symmetry considerations, the 4 p_z contribution should not be neglected. However it cannot be separated from the $3d_{z^2}$ contribution in the anisotropic hyperfine coupling terms. Kawamura[9] suggests that, because of its diffuseness, the $4p_z$ orbital should have a small contribution to the experimental anisotropic term so that it could be neglected in the estimation of the $\rho(Co,d_{z^2})$ density.

Unpaired Electron Distribution on the Ligand Orbitals. The unpaired electron distribution on the ligand orbitals can be correlated with the corresponding hyperfine coupling parameters as follows:

$$A_\parallel = a + 2(a_d + a_\sigma - a_\pi) \quad (3a)$$

$$A_\perp = a - (a_d + a_\sigma - a_\pi) \quad (3b)$$

a is the isotropic term, a_σ and a_π are the anisotropic terms, arising from an unpaired electron density in either a σ or π ligand orbital, and a_d is a dipolar term given by $g_e\beta_e g_n\beta_n/R^3$, where R is the metal–ligand distance.

The hyperfine parameters reported in Table I for the six ^{19}P nuclei are almost isotropic. So most of the electron–nuclear interactions arise from a contact term due either to a contribution of the 4s phosphorus orbital or to a spin-polarization term. For a cobalt–phosphorus distance of 2.2 Å,[22] the a_d dipolar term is about 10^{-4} cm^{-1}; a value close to the experimental resolution; a_σ and a_π should not exceed such a value, suggesting that the unpaired electron density has a very small extension toward the 3p phosphorus orbitals. Neglecting the inner-shell spin polarization, the unpaired electron density on the 3s phosphorus orbital could be estimated according to

$$a(P) = Q_V(P)\ \rho(P,s)$$

The literature[26] gives $Q_V(P) = 4440 \times 10^{-4}$ cm^{-1}. $\rho(P,s)$ is thus about 0.009. Nevertheless, there is no good reason to ignore spin polarization, and both phenomena certainly take place.

The fluorine hyperfine parameters are rather high although fluorines are linked to cobalt atoms via phosphorus atoms. This may be attributed to the large value of the $Q_V(F)$ isotropic term which is equal to $17\,600 \times 10^{-4}$ cm^{-1}.[26] Even a very small spin density in a 2s ^{19}F atomic orbital leads to a consistent isotropic hyperfine parameter. In our case, the $\rho(F,s)$ density is estimated as 0.0003.

The a_d dipolar term expected for a fluorine–cobalt distance of about 3 Å[22] is 10^{-4} cm^{-1}, a value in agreement with the anisotropy revealed by ENDOR experiments.

Table II. Wave Function Coefficients for the Semioccupied Molecular Orbital of the Radical Anion $[[CH_3N(PF_2)_2]_3Co_2(CO)_2]^-$ with a Comparison between ESR Results and Extended Hückel Calculations

nucleus	AO	ESR results	EH calculations
cobalt	4s	0.08–0.11	0.15
	$4p_z$		0.29
	$3d_{z^2}$	0.62	0.52
phosphorus	2s	0.09	0.08
	2p		0.10
fluorine	2s	0.02	0.01–0.02

Table III. Unpaired Electron Distribution in Cobalt Carbonyl Derivative Radical Anions

complex	$\rho(Co,s)$	$\rho(Co,d_{z^2})$	$\rho(E,s)$	$\rho(E,p_z)$	ref
$[Co_2(CO)_6(P\text{-}n\text{-}Bu_3)_2]^-$	0.009–0.015	0.31	0.014	0.09	9
$[Co_2(CO)_6(P(OMe)_3)_2]^-$	0.009–0.015	0.32	0.026	0.02	9
$[Co_2(CO)_6(As\text{-}i\text{-}Bu_3)_2]^-$	0.010–0.016	0.31	0.018	0.03	9
$[Co_2(CO)_2(CH_3N(PF_2)_2)_3]^-$	0.006–0.013	0.38	0.009		*a*

[a] This work.

The calculated electron densities on both phosphorus and fluorine ligands suggest that the unpaired electron is poorly delocalized on the fluorophosphine equatorial ligands. Owing to the estimated unpaired electron density on cobalt nuclei, the contribution of the carbonyl axial ligand should be rather important.

Extended Hückel Calculation: Comparison with Experimental Data. Extended Hückel calculations were carried out in order to get a better description of the molecular orbitals in such complexes. They were performed on the neutral parent complex whose structure is known.[22] The cobalt–cobalt bond was chosen as the z axis (I). From these calculations, the LUMO appears as the

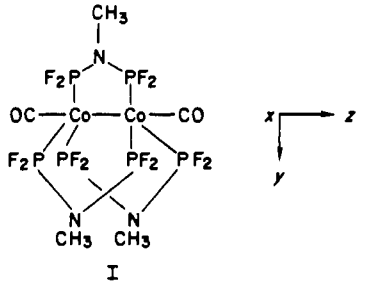

I

antibonding combination of the d_{z^2} cobalt orbitals. The 4s, $4p_z$, and $3d_{z^2}$ cobalt orbitals contribute to this σ^* level with 0.15, 0.29, and 0.52 wave function coefficients, respectively. The most important ligand contribution comes from the axial carbonyls, via their σ molecular orbitals. The wave function coefficients for the 2s and $2p_z$ carbon orbitals are 0.24 and 0.19, respectively. For the $2p_z$ oxygen orbitals, the coefficient is 0.13. The wave functions have little extension on the equatorial phosphines, with coefficients around 0.10 for the 2p phosphorus orbitals overlapping with the cobalt orbitals.

According to the overlap integrals, it is interesting to notice that the overlap between the $4p_z$ and $3d_{z^2}$ cobalt orbitals and the σ carbonyl orbital is quite large, $S(3d_{z^2},\sigma) = 0.13$ and $S(4p_z,\sigma) = 0.35$, in comparison with those between the cobalt d_{z^2} orbital and the phosphorus p orbital, $S(3d_{z^2},2p) = 0.05$. All the electronic density is concentrated along the z axis.

The calculated wave function coefficients are in good agreement with those obtained from ESR experimental data (Table II). The d_{z^2} coefficient evaluated from ESR data seem to be overestimated because the $4p_z$ contribution was neglected, as pointed out before.

Kawamura and co-workers have published ESR studies[6,9] of other cobalt carbonyl derivative radical anions in which the axial carbonyls were replaced by phosphites, phosphines, or arsines. Our

Table IV. Extended Hückel Parameters Used for the Calculations

atom	orbital	H_{ii}, eV	ξ_1[a]	ξ_2[a]
Co	4s	−9.21	2.0	
	4p	−5.29	2.0	
	3d	−13.18	5.55 (0.5680)	2.10 (0.6060)
P	3s	−18.6	1.6	
	3p	−14.0	1.6	
F	2s	−40.0	2.425	
	2p	−18.1	2.425	
O	2s	−32.3	2.275	
	2p	−14.8	2.275	
N	2s	−26.0	1.95	
	2p	−13.4	1.95	
C	2s	−21.4	1.625	
	2p	−11.4	1.625	
H	1s	−13.6	1.3	

[a] Two Slater exponents are listed for the 3d functions. Each is followed in parentheses by the coefficient in the double-ζ expansion.

results are quite consistent with theirs (Table III).

We must notice however that Kawamura's radical was very unstable so that it was not possible to obtain a liquid-solution spectrum at room temperature. The isotropic hyperfine tensor value was unknown, leading to an ambiguity concerning the sign of $A_\parallel$ and $A_\perp$. Assuming a d_{z^2} ground state, they considered $A_\parallel$ as positive and $A_\perp$ as negative. Our results provide support to such an interpretation.

The main difference is that they observed a significant anisotropy of the phosphorus coupling constant whereas, in our work, the phosphorus coupling is isotropic within the experimental resolution. This could be expected since the phosphorus atoms are in an axial position and can therefore contribute to the σ^* molecular orbital via their $2p_z$ orbitals.

Experimental Section

The radical anion $[[CH_3N(PF_2)_2]_3(Co)_2(CO)_2]^-$ was prepared according to the previously described procedures.[11,17] X-Band ESR and ENDOR experiments were performed on a Bruker 220 D spectrometer equipped with a Bruker ENDOR accessory and an Oxford Instrument ESR 9 continuous-helium-flow cryostat. The extended Hückel calculations were performed using the ICON, version 8 program. The atomic orbitals are simple Slater-type orbitals except for cobalt 3d orbitals where a linear combination of two Slater functions was chosen. The parameters for all atoms used are listed in Table IV. The Wolfsberg–Helmholz proportionality constant k was set at 1.75.

Acknowledgment. We thank Prof. R. B. King (Athens, GA) and Dr. N. El Murr (Nantes, France) for preparing the radical anion. We are indebted to Dr. D. Gourier (Paris, France) for ENDOR experiments. Extended Hückel calculations were performed at the CIRCE (Orsay University, France).

Registry No. $[[CH_3N(PF_2)_2]_3Co_2(CO)_2]^-$, 73988-94-0.

Contribution from the Department of Chemistry, New Mexico State University, Las Cruces, New Mexico 88003

Kinetic Aspects of the Iron(III)- and Iron(II)–Tetrakis(*N*-methylpyridinium-4-yl)porphine Systems

G. A. Tondreau and R. G. Wilkins*

Received December 2, 1985

The spectra of monomeric and dimeric iron(III) and monomeric iron(II) complexes of TMPyP were examined (TMPyP = tetrakis(*N*-methylpyridinium-4-yl)porphine). The kinetics of interconversion of $Fe(TMPyP)(OH)^{4+}$ and $(TMPyP)Fe–O–Fe(TMPyP)^{8+}$ have been studied by dilution relaxation at pH 7.0–8.5, I = 0.05 M, and 25 °C. The formation of the dimer is from $Fe(TMPyP)(OH)^{4+}$ and $Fe(TMPyP)(H_2O)_n^{5+}$ ($k = 9 \times 10^2$ M^{-1} s^{-1}). Reduction of the iron(III)–TMPyP complexes by ascorbate is biphasic. The fast step leads to a bisadduct. The slow step is first-order ($k = 4 \times 10^{-3}$ s^{-1}), independent of ascorbate concentration. The reaction of $Fe(TMPyP)^{4+}$ with O_2 is third-order ($k = 3.5 \times 10^2$ M^{-2} s^{-1}) and with H_2O_2 is second-order ($k = 6.0 \times 10^6$ M^{-1} s^{-1}) at pH 8.0. The iron(II):oxidant mole ratio is 4:1 for O_2 and 2:1 for H_2O_2, and the product first formed is monomeric iron(III)–TMPyP. The mechanisms are discussed.

Introduction

The metalloporphyrin ring is an integral feature of a vast number of biological materials containing iron. There have therefore been a large number of studies of metal complexes of both naturally occurring porphyrins and synthesized derivatives.[1] The kinetics of substitution, redox, and photochemical reactions of metalloporphyrins have been amply studied,[2] and the results have relevance to the biological systems. Water solubility is conferred on the porphyrin by substituting hydrophilic cationic and anionic groups on the periphery of the porphyrin, and a number of these porphyrins and their metal complexes have been studied.[2]

We have previously examined the thermodynamic and kinetic aspects of the equilibrium between the monomer and dimer forms of the iron(III)–tetrakis(*p*-sulfonatophenyl)porphine complex (I, X = CSO_3^-, ligand abbreviated TPPS).[3] In order to determine

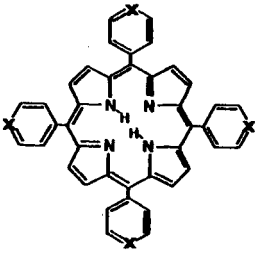

I

the effect of the porphyrin structure on this and other properties, we turn our attention to the iron–tetrakis(*N*-methylpyridinium-4-yl)porphine complex (I, X = NCH_3^+, ligand abbreviated TMPyP). The diagnosis of species present in iron(III) and iron(II) mixtures with TMPyP is difficult, and it is not surprising that

(1) *Porphyrins and Metalloporphyrins*; Smith, K. M., Ed.; Elsevier: Amsterdam, 1975. *The Porphyrins*; Dolphin, D., Ed.; Academic: New York, 1978. *Iron Porphyrins*; Lever, A. B. P., Gray, H. B., Eds.; Addison-Wesley: Reading, MA, 1983.
(2) Lavallee, D. K. *Coord. Chem. Rev.* **1985**, *61*, 55.
(3) El-Awady, A. A.; Wilkins, P. C.; Wilkins, R. G. *Inorg. Chem.* **1985**, *24*, 2053.

0020-1669/86/1325-2745$01.50/0